euspen's 23rd International Conference & Exhibition, Copenhagen, DK, June 2023
www.euspen.eu

Towards miniaturised instrumentation realised via metasurfaces

J. G. Kendrick[1], A. J. Henning[1*], H. Martin[1], J. Williamson[1], D. Tang[1], N. Sharma[1], X. Jiang[1]

[1]*Centre for Precision Technologies, University of Huddersfield, UK, HD1 3DH*

**A.Henning@hud.ac.uk*

Abstract

The miniaturisation of optical instrumentation is a vital step in order to produce sensors in a form that can be integrated into manufacturing lines, providing the feedback required to control and optimise such processes. While incremental progress has been achieved by using conventional optical technologies, a markedly different route is needed to achieve the step-change in size and weight reduction required. Metasurfaces, which are nanostructured surfaces that can simultaneously manipulate the phase, polarisation and amplitude of light, offer a new basis upon which truly miniaturised optical instrumentation can be realised.

Here we present our initial work on using metasurfaces to miniaturise a single-shot dispersive profile interferometer (SDPI), which is a line profile measuring instrument designed for the measurement of moving substrates in roll-to-roll applications. A key optical element in the SDPI is a line spectrometer, which provides for the spectral evaluation of light to be measured for each point along the entrance slit. Current line spectrometers are large and bulky, which creates a significant impediment to compactness. However, we have designed a metasurface that allows the necessary optical operations to be carried out in an ultra-compact and lightweight form. The metasurface has been fabricated by etching pillars into a layer of GaN on an Al_2O_3 substrate. We present our results covering the performance characterisation of this metasurface spectrometer and the subsequent steps towards developing an instrument based around it. The experimental results will demonstrate a significant reduction in size and weight compared to a comparable approach based on conventional optics with improved optical functionality.

Keywords: Metrology, Metasurfaces, Optical Instrumentation

1. Introduction

In order to realise the vision of 'Industry 4.0' [1], where smart and autonomous processes are used in production lines to produce bespoke items 'right first time', there is a need to produce sensors in a form that can deliver in-line and in-process measurements and provide the feedback that can be used to make any necessary adjustments to the manufacturing processes [2-4]. This approach will not only lead to reduced scrappage rates, saving the time and energy that would have gone into making the rejects, but will also save the time and effort needed to hone the manufacturing processes each time a new object is made.

Optical sensors are ideal candidates for this task, as they can provide non-contact, high speed, and high precision measurements of surfaces, however their large size and weight is a barrier to their deployment. Unless they are created in a sufficiently light and compact form their use would interfere with the production processes that they are meant to be monitoring, or they may not physically be able to be located where the measurements need to be taken. While efforts have been made to reduce the size of optical instrumentation for just such tasks [5] progress is incremental, with the traditional approach of using refractive elements to manipulate the light being a limiting factor. An alternative approach by which ultra-compact instrumentation can be created is the exploitation of the emerging technology of optical metasurfaces [6,7].

Metasurfaces use arrays of nanostructures, each of which is commonly termed a 'meta-atom', or 'meta-molecule', to manipulate light as it propagates through the structure [8]. By varying the form of the meta-atoms across a surface exquisite control over the phase, amplitude, and polarisation of light can be achieved and, as the manipulation of the light is carried out using a layer of structures whose height is on the order of a wavelength, the metasurface can provide the same functionality as traditional optical elements but without the associated size or weight. By replacing traditional elements with metasurface equivalents, or by creating metasurface elements that combine the function of several traditional elements, a much less bulky instrument can be formed.

In the following we present our initial efforts to create a metasurface spectrometer specifically designed for use within a single-shot dispersive profile interferometer (SDPI) [9,10], an interferometric optical line profile measuring instrument. This instrument provides a line measurement by using a spectrometer that takes the light passing through a slit and, for each point along it, splitting it into a separate spectrum. By analysing the fringes generated, the height along a line of the scattering surface is obtained. While we retain refractive optics in part of the system, a significant portion of the instruments size and weight can be removed by implementing a metasurface based spectrometer instead of one in the conventional form.

2. Metasurfaces as a technology enabling miniaturisation

There are several different types of meta-surfaces that have been demonstrated, such as Huygens [8] or Pancharatnam-Berry [11] metasurfaces, but it is the truncated waveguide form that is used here. Specifically, in this work the nanostructures take the form of dielectric pillars made from GaN, whose radii are changed to vary the phase delay that the light experiences as it passes through the metasurface. Structures of this form are chosen as the rotational symmetry of the meta-atoms will minimise any variation with the polarisation of incident light. An

SEM image of one of these structures is shown in fig 1(a). The GaN pillars are etched from the surface of a $4.5\ \mu m$ layer of GaN on a $430\ \mu m$ thick wafer of Al_2O_3. These pillars are 750 nm high and are arranged in a square lattice of period 450 nm, with the radii being changed from 70 nm to 170 nm in 10 nm steps. When the incident light has a wavelength of 660 nm, this set of pillars allows the phase delay the light experiences to be varied over a 2π range, as shown in fig 1(b). The ability to vary the phase delay by this amount means an arbitrary incident wavefront can be converted into an arbitrary outgoing wavefront, modulo 2π. It should be noted that it is important that the spacing of the meta-atoms is sub-wavelength, otherwise light will be diffracted into unwanted directions.

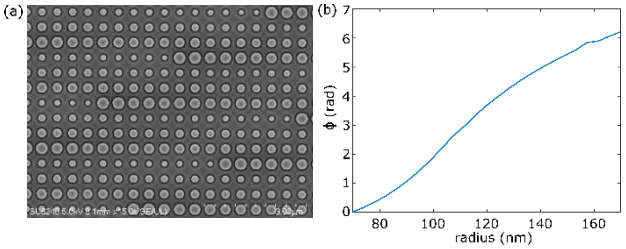

Figure 1. Part (a) shows an SEM image of the GaN pillars that make up the metasurface spectrometer in this work while part (b) shows the relative phase after passing through arrays of pillars of differnt radii (when $\lambda = 660$ nm).

A line spectrometer composed of traditional optical elements takes up a significant portion of the size and weight of the SDPI instrument. By replacing this with a spectrometer based on a metasurface a far more compact instrument can be created. The basic version of the metasurface spectrometer used here just takes the form of a metalens, but one that focusses a collimated beam propagating perpendicular to the metasurface to an off-axis point [12]. This functionality is designed for a single wavelength, ideally chosen near the middle of the range of wavelengths the spectrometer will cover. At this wavelength, the metasurface modifies the phase of the wavefront so that just after the metasurface it is [13]

$$\phi(x,y) = -\frac{2\pi}{\lambda}\left(\sqrt{(x-D)^2+y^2+z^2}-f\right) \qquad (1)$$

Where f is the focal length of the lens and D is the shift along the x axis where the focal point is found. This corresponds to

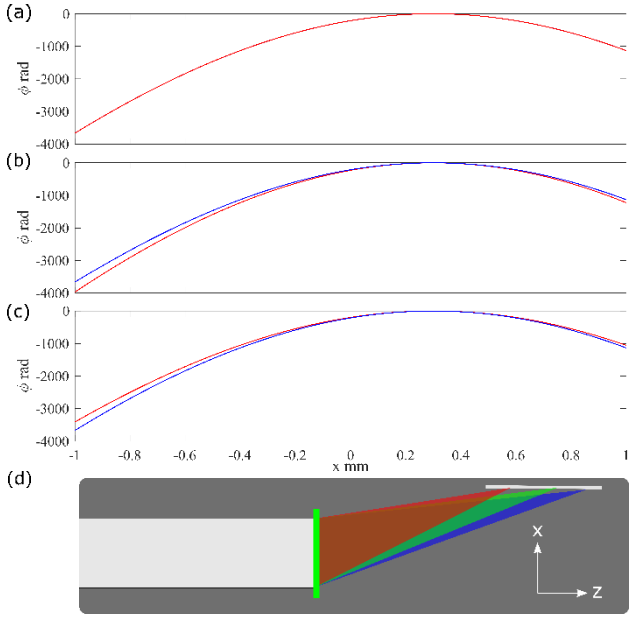

Figure 2. The ideal phase delay to focus light to the point x= 0.3 mm, y =0, z = 2 mm is shown by the red lines in parts (a), (b) and (c) for the wavelengths 660 nm, 610 nm, 710 nm respectively. In each case the blue line shows the phase delay imparted by the surface. Part (d) illustrates the manner in which the light is separated by wavelength.

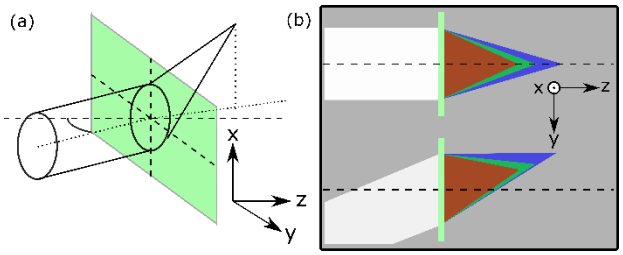

Figure 3. Part (a) illustrates that when the incident beam of light is rotated around the x-axis the focal points generated move off the y=0 plane. Part (b) shows the y-z view as the incident beam angle is changed.

part of a spherical wavefront centred on the desired focal point. However, the metasurface created from the GaN pillars only satisfies this equation at the design wavelength. Away from this point both changes in the wavelength, and the wavelength dependence of the phase delay that the pillars impart, mean that the light is focussed to a different point in space. This is illustrated in fig. 2. In parts (a), (b) and (c) the red line represents the ideal phase after the surface, as given by eq. (1), that would lead to light with a wavelength of 660 nm, 610 nm and 710 nm respectively to be focussed to a point x= 0.3 mm, y =0, z = 2 mm, (where top of the metasurface lies in the plane z=0). The blue line, however, gives the unwrapped phase that is found after the light has passed through a metasurface that was designed to focus light of wavelength 660 nm to that point. While the red and the blue lines match well in fig2(a), (where the light corresponds to the design wavelength), in fig2(b) where the wavelength is shorter ($\lambda = 610$ nm) the variation in phase across the surface is less than that given by eq.(1), shifting the focal point further away from the surface. For the longer wavelength, shown in fig.2(c) ($\lambda = 710$ nm), the variation in phase is more than that given by eq. (1), focussing the light closer to the surface. By placing a detector in the correct location this shift in the location of the focal spot with wavelength allows a spectrometer to be created, as illustrated in fig 2(d).

While this metasurface takes the light from a collimated beam and separates and focusses the different wavelengths to different positions along a line, this alone is not sufficient for the SDPI application. However, when the incident beam of light is tilted so that it makes an angle with the x-z plane, as shown in fig. 3(a), the location of the focal points shifts away from the $y = 0$ plane. Thus, light incident at an angle will be focussed to a different set of points in space, and while aberrations will be present, this can be used to create the line spectrometer needed for the SDPI instrument, as shown in fig. 3 (b).

3. Single-shot dispersive profile interferometry

A typical realisation of the SDPI technique is illustrated in fig. (4). Light from an extended spatially incoherent broadband light source is divided into two paths, one of which reimages the source onto a reference mirror and the other onto a plane in the object space. The surface being measured is placed in the vicinity of the focal plane in the object space, and light scattered from it is collected by the objective lens and combined with the light scattered from the reference mirror. The objective lens is combined with a tube lens to allow an image to be formed. A narrow slit is placed on the conjugate focal plane of the image of the source, with the light that passes through the slit being analysed using a line spectrometer. When the surface of the measurand is away from the focal plane in the object space the image of it will be de-focussed, reducing the lateral resolution of the measurement, however the broadband interferometric

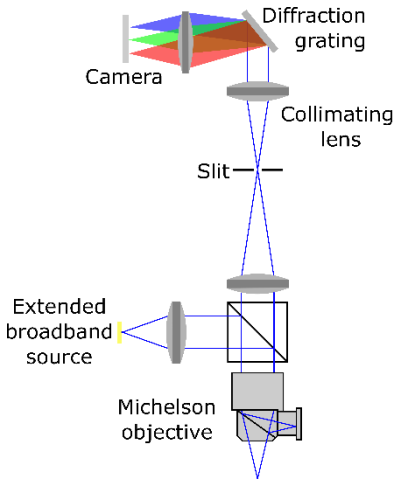

Figure 4. A schematic of a typical SDPI instrument.

measurement approach taken allows the distance to the surface to be measured albeit, when defocussed, mixing light from a larger area of the surface in the signal.

A slit is used so that the height of the surface along a profile can be obtained in a single measurement. The light from each point on the slit is split into its spectrum in the direction perpendicular to the slit, for instance, through the use of a diffraction grating. This then forms a 2D signal on a detector; in one direction each row of pixels corresponds to a different point along the slit, while in the second direction the column of pixels corresponds to the different wavelengths of light at each of those points.

On each pixel of the detector the signal measured is the interference between the light scattered from the reference mirror and the light scattered from the measurand, with the phase difference between the light following each of the paths being dependant on the difference in optical path length and the wavelength of the light [7], with the intensity measured, I_{meas}, being given by

$$I_{meas}(x,k) = I_1(x,k) + I_2(x,k) + 2\sqrt{I_1(x,k)I_2(x,k)}\cos\big(k\Delta l(x)\big) \quad (2)$$

Where $I_1(x,k)$ is the intensity of the light from the reference path for the position x on the slit, and with a wavenumber k, where $k = 2\pi/\lambda$. $I_2(x,k)$ corresponds to the intensity of the light from the measurement path and Δl is the path difference between light propagating in the reference and the measurement arms. The first two terms provide a constant background signal while the third term corresponds to the interference between the two beams. For each column of pixels, which corresponds to the different wavelengths of light incident on the same point on the surface, the value of $\Delta l(x)$ is constant, so the variation in the signal arises from changes in I_1 and I_2 and the variation in k. For simplicity it will be assumed that I_1 and I_2 are constant with respect to k as, while this is unlikely to be true in practice, by measuring the envelope on the sinusoidal variation and normalising, that variation can be compensated for in most cases. Thus, the variation in I_{meas} is due to the $\cos(k\Delta l)$ term and, if the spectrometer varies k linearly across the detector, the signal will form a sinusoid. A method such as that given in [14] can be used to calculate the phase of the signal and, after unwrapping, the gradient of the phase will allow Δl to be obtained.

The metasurface as described above is designed to take a collimated beam of light as the input, and so an additional element needs to be included to first convert the light that passes through the slit into this form. Thus, while the function of the diffraction grating and the imaging lens is combined by the metasurface, the collimating lens shown in fig. 4 still needs to be retained. The collimating lens will take the light from each point along the slit and collimate it, but with each point on the slit producing a beam that is propagating at a different angle, which is exactly the case that is being considered with the metasurface in section 2. When considered in this manner, the maximum useable angle for which the metasurface provides sufficiently unaberrated focal points will relate directly both to the length of slit that can be used, and parameters of the collimating lens.

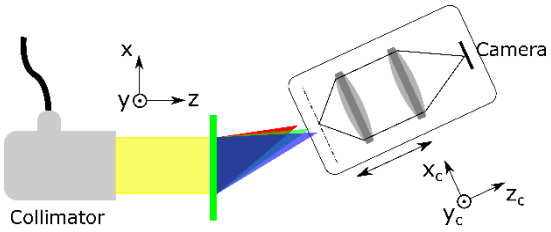

Figure 5. The experimental setup used to characterise the sample. Narrow bandwidth light is passed through the metalens, and the microscope is scanned to reimage the light focussed after the metalens.

4. Results from the manufactured metasurface

The effect of the metasurface was verified using the experimental setup illustrated in fig. 5. As the metasurface is designed to produce a focal spot that is approximately the same size as a pixel on a detector that is to ultimately be used with it, in this case 5 μm, if the focal spots are measured by scanning a camera through the focal region there will not be sufficient resolution to characterise them well. For this reason, a microscope mounted on a translation stage was built to allow a magnified image of the focal plane to be produced on the camera. For each focal point 250 images were taken with the microscope being moved a distance of 200 nm between each image. The microscope uses a camera with a pixel size of 3.45 μm, and magnifies the image on the focal plane 20 times.

To create the focal point to be measured, the light from a white light source is passed through an acousto-optic tuneable filter (AOTF) which only allows light in a narrow band of wavelengths to be passed. This is coupled into an optical fibre, before being collimated using a reflective collimator. This beam passes through the metalens to produce the focal point which is then measured. This measurement is repeated 8 times with the central wavelength of light passed by the AOTF being changed from 525 nm to 700 nm in 25 nm steps. This is then repeated with the angle between the normal to the substrate and the direction of propagation of the collimated beam being changed from -2 degrees to 2 degrees in 1 degree steps.

Figure 6 shows a selection of images of the focal points as the angle and the wavelength are changed. These are recorded when z_c = 9.6243 mm, 9.1925 mm and 9.6256 mm for parts (a), (b) and (c) respectively. It should be noted that the camera co-ordinate system (x_c,y_c,z_c) is not the same as that used to describe

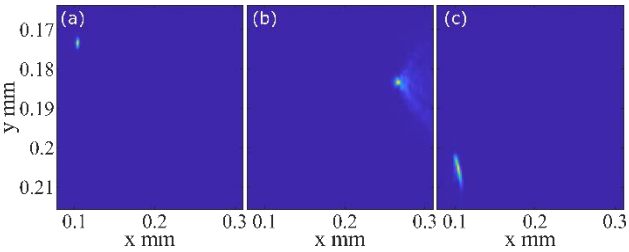

Figure 6. Images recorded when (a) $\lambda = 675$ nm, incidence angle of 0 degrees and where $z_c = 9.6243$ mm (b) $\lambda = 550$ nm, incidence angle of 0 degrees and where $z_c = 9.1925$ mm (c) $\lambda = 675$ nm, incidence angle of 2 degrees and where $z_c = 9.6256$ mm.

the metasurface, as illustrated in fig. 5. The focal point shifts between parts (a) and (b) due to a change in wavelength, while the change in position between parts (a) and (c) is due to a change in the incidence angle. It should be noted that, as well as aberrations being seen that increase the further away from the ideal design parameters of the metalens ($\lambda = 660$ nm, and the light propagating perpendicular to the surface of the substrate), these images slice through the focal points at an angle. However, it can still be seen the focal points move in the manner expected. The alignment is not perfect, as ideally the only change in location between parts (a) and (b) would be a shift along the x-axis, and as the angle was set manually by hand, it is likely that there will be some error. This will be addressed in further work on the characterisation of the performance of these structures.

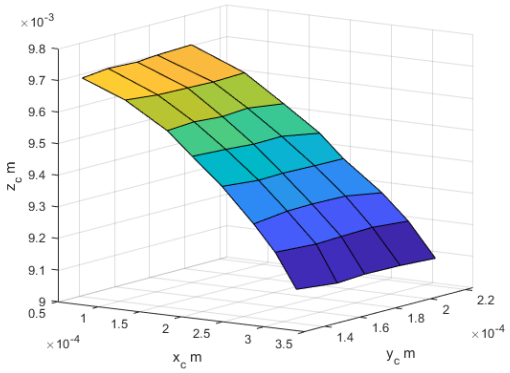

Figure 7. A plot of the surface the focal points lie on as the wavelength is changed from 525 nm to 700 nm in 25 nm steps, and the angle the incident beam makes with the metasurface is changed from -2 degrees to 2 degrees in 1 degree steps.

While a measurement of only 8 wavelengths, and five angles, gives quite a coarse indication of the performance of the metasurface, it does allow the surface on which the focal points move to be mapped out, as is shown in fig 7. The significant movement of the focal spot with both changes in the wavelength and the incidence angle does indicate that this metasurface provides a viable candidate for the basis of a spectrometer for the SDPI instrument. The shift in the focal point is, in part, dependent on the focal length of the metasurface. If the location of the focus at the design wavelength of 660 nm was changed, then so would be the size of shift in the focal point as the wavelength changes, allowing the resolution to be adjusted. It should be noted that, for each different angle of incidence, while the position changes with wavelength the lines that the focal points move along are not parallel for different incident angles. However, as each wavelength and angle focusses light to a different point, this effect can be characterised and compensated for when the full SPDI instrument is built.

5. Summary, Conclusions and Future work

We have developed a metasurface that combines the function of the dispersive and focussing elements of the SDPI's spectrometer, and we have measured its effect on a collimated beam of light, both square on, and at an angle to, the optical axis in order to verify its suitability for this task. This is the first step in reducing the size of this instrument, a step that will lead to the creation of a highly integrable instrument that can be used for in-line and in-process measurements, and allow it to be used in cases where its current form is prohibitive.

While the focal points are aberrated away from the design wavelength, they are still sufficiently well-formed that a highly useable spectrometer can be formed.

The next step in the development of the metasurface is to combine the function demonstrated here with the function of the collimating lens that is found after the slit in the current SDPI. This will remove a further bulky element from the system and leave the spectrometer consisting of just the metasurface element and the detector. The metasurface based version will not be quite equivalent to one using a refractive lens, as there will be a wavelength dependent nature to this additional function added to the metasurface. This is likely to increase the change in position of the focal spot produced after the lens.

While it is important to characterise the focal spots that are produced when light passes through the surface, when the metasurface is used to realise a spectrometer the detector that will be combined with the metasurface will detect light on a plane. As the focal points do not lie on a plane they will not all coincide with this, thus, the defocussed focal points across the plane need to be considered, and will be examined in further work.

Acknowledgements

The authors gratefully acknowledge the UK's Engineering and Physical Sciences Research Council (EPSRC) funded programmes EP/T02643X/1, and EP/P006930/1 along with the UK's Royal Academy of Engineering and Renishaw PLC who sponsor Xiangqian Jiang's REng/Renishaw Research Chair.

References

[1] Henning, K., Wolfgang, W. and Johannes, H., 'Recommendations for implementing the strategic initiative INDUSTRIE 4.0'. Final report of the Industrie, 4, p.82. (2013).

[2] Gao, W., Haitjema, H., Fang, F. Z., Leach, R. K., Cheung, C. F., Savio, E., & Linares, J. M. On-machine and in-process surface metrology for precision manufacturing. CIRP Annals, 68(2), 843-866. (2019).

[3] Jiang X. Precision surface measurement. Phil Trans R Soc A. 370:4089–4114. (2012)

[4] Osten W. Optical metrology: from the laboratory to the real world. In Computational Optical Sensing and Imaging (pp. JW2B-4). Optical Society of America. (2013).

[5] Santoso T, Syam WP, Darukumalli S, Cai Y, Helmli F, Luo X, Leach R. On-machine focus variation measurement for micro-scale hybrid surface texture machining. The International Journal of Advanced Manufacturing Technology. 109(9):2353-64. 2020

[6] Henning A.J., Townend D., Martin H., Jiang X.. Metasurface-based ultracompact instrumentation to support future smart manufacturing. In Optics and Photonics for Advanced Dimensional Metrology II (p. PC1213706). SPIE (2022)

[7] Jiang X., Henning A.J. Precision metrology: from bulk optics towards metasurface optics. Contemporary Physics.62(4):199-216. (2021).

[8] Yu N, Capasso F. Flat optics with designer metasurfaces. Nature materials. 13(2):139-50. (2014)

[9] Tang D, Gao F, Jiang X. On-line surface inspection using cylindrical lens–based spectral domain low-coherence interferometry. Appl Opt. 53(24):5510–5516 (2014)

[10] Guo T, Zhao G, Tang D, et al. High-accuracy simultaneous measurement of surface profile and film thickness using line-field white-light dispersive interferometer. Opt Lasers Eng. 137:106388. (2021)

[11] Chen WT, Zhu AY, Capasso F. Flat optics with dispersion-engineered metasurfaces. Nature Reviews Materials. 5(8):604-20. (2020)

[12] Zhu, Alexander Y., et al. Ultra-compact visible chiral spectrometer with meta-lenses. Apl Photonics 2.3 036103. (2017)

[13] Guo Q, Shi Z, Huang YW, Alexander E, Qiu CW, Capasso F, Zickler T. Compact single-shot metalens depth sensors inspired by eyes of jumping spiders. Proceedings of the National Academy of Sciences. 116(46), (2019)

[14] Takeda, M., Ina, H., & Kobayashi, S. Fourier-transform method of fringe-pattern analysis for computer-based topography and interferometry. JosA, 72(1), 156-160. (1982).